Int. J. Electrochem. Sci., 7 **(2012)** 150 - 166

International Journal of
ELECTROCHEMICAL
SCIENCE
www.electrochemsci.org

Carbon Film Electrodes as Support of Metallic Particles

S. J. Figueroa Ramírez, M. Miranda-Hernández[*]

Dpto. Materiales Solares, Centro de Investigación en Energía. Universidad Nacional Autónoma de México. Apartado Postal 34, Temixco, Mor., México. CP 62580.
[*]E-mail: mmh@cie.unam.mx

Received: 2 November 2011 / *Accepted:* 11 December 2011 / *Published:* 1 January 2012

The commercial carbon black is used as a film electrode (nCFE), and as support of the copper and palladium particles. The electrodes Cu/nCFE, with different quantities of copper was evaluated for the electrochemical reduction of CO_2 in 1M $KHCO_3$ by means cyclic voltammetry, and exhibited a good behavior as catalysts. The morphology of the electrodes had an important influence in the catalytic process. On the other hand, the cyclic voltammetry studies allowed to define a specific potential range for palladium electrodeposition without hydrogen evolution (-0.09 to -0.17 V vs. SCE), and by means of anodic stripping voltammetry it was possible to evaluate the corresponding mass of metallic palladium with and without hydrogen discharge. The carbon black was used without purification and FTIR analysis shows they surface chemical composition (C-O, C=O, CF_2, CF, S-O, C-O-C). These groups provide a degree of chemical reactivity. However, they did not affect the electrochemical deposit of copper and palladium; they are not electroactive in ammonia acidic and basic systems. The SEM images showed the morphology of copper and palladium particles. The copper dispersion on the surface of carbon electrode was analyzed by energy dispersive spectrometer (EDS). The hydrogen discharge reaction has an important influence in the palladium particles morphology. The size of the palladium particles are about 31 and 34 nm estimated by analysis XRD.

Keywords: Carbon films electrodes, Copper and palladium particles, Carbon black film, Support for catalysts

1. INTRODUCTION

The formation of catalytically active metal particles on a solid support is especially important for heterogeneous catalysis. Usually, in practice noble metal electrodes are prepared with small amounts of these metals, highly dispersed on a low cost conductive substrate. This provides a large surface area which increases the rate of reaction [1]. Carbon black is an attractive material as support of catalysts; due to their physical and chemical surface properties. The large surface area, pore size and their distribution are appropriate to facilitate the diffusion of reactants and products to and from the

surface. This material becomes chemically interesting because of the presence of the functional groups on its surface, the acid-base character the chemical activity displayed, more or less depending the chemical environment and use in different applications. This material becomes chemically interesting because of the presence of functional groups on its surface. The acid-base character and chemical activity displayed depends on the chemical environment of its uses and applications. The surface chemical activity is precisely one of the limitations for its use as catalyst supports, due to its interference with the study process [2-8]. Although the presence of these functional groups does not necessarily lead to a chemical reaction on the surface, it affects physical adsorption [9-11].

In cases, where the chemical adsorption is important carbon materials are good alternative. In the case of electrochemical reduction of CO_2 on polycrystalline copper electrode, CO is an important intermediary product, which adsorbs on the surface of the catalyst causing its passivation or poisoning, slowing down the catalytic activity [12, 13]. An alternative is to disperse copper particles on the carbon support, in order to increase the catalytic activity of copper electrode, considering that CO has affinity by carbon.

On the other hand, the high catalytic activity of palladium is obtained by modifying solid surfaces with micro-or nanoparticles dispersed of this metal [14, 15]. Palladium is the most studied metal in the hydrogen interaction [16, 17]. Among the various noble metals palladium has the unique property to adsorb hydrogen within its lattice [18, 19]. It is important to say that hydrogen discharge potential occurs under conditions very close to the palladium deposition [20-22]. This complicates the process efficiency and the morphological quality of the palladium deposit, and it has been reported that these defects in the morphology, affect its catalytic ability.

An alternative is to disperse palladium particles on a matrix to ensure its catalytic ability, but still there is the problem of simultaneous hydrogen discharge reaction on the palladium particles deposited at the early stage. Considering that currently the carbon black is commercially available (in different forms and varieties) and the cost is relatively low compared with other materials, it becomes an attractive alternative for the direct application in the practical point of view.

There are only few reports where the commercial carbon black were used as catalytic supports, without prior purification treatments. This study presents the use of carbon black, from commercial origin, as film electrode that supports particles of both copper and palladium, and they were evaluated as catalysts in the electrochemical reduction of CO_2 in the case of copper. In the case of palladium we obtained the dispersed particles at a potential range without the influence of the hydrogen discharge.

2. EXPERIMENTAL

2.1 Preparation of the Carbon Film Electrodes (nCFE)

The film was prepared from a solution that containing 16 mg of nanostructured carbon black, 0.16 ml Nafion, and 0.64 ml isopropyl alcohol, and it was agitated for 30 minutes in an ultrasonic bath. The size of particle of carbon black is 5 nm, surfaces area (BET) 246 m^2/g, and 0.01% sulphur (Columbian Chemical Company)

2.2 Scanning Electronic Microscopy (SEM)

The morphology of nCFE, copper and palladium particles was evaluated using high resolution scanning electron microscope (FE SEM Hitachi S-5500). The dispersion of copper on the surface of carbon electrode was analyzed by energy dispersive spectrometer (EDS) by using Scanning Electron Microscope (LEO-1450VP).

2.3 Fourier transform infrared (FTIR) spectroscopy

In order to describe the chemical surface composition of the carbon film electrode (nCFE), FTIR analysis was carried out. IR spectra were acquired using a Fourier transform infrared (FTIR) spectrometer Bruker Equinox 55 S. The samples were pellets, were prepared by mixing the potassium bromide (KBr, 0.91%) with carbon black (0.09%) and carbon film powder (0.09%), respectively, and it was applied great pressure. In the case of Nafion was prepared a KBr pellet, then is placed a drop of Nafion on the pellet and allowed to dry.

2.4 X Ray diffraction (XRD)

The diffractograms of palladium particles were obtained at room temperature using Cu Kα radiation λ=1.54Å in a Rigaku X ray diffractometer (Model Dmax 2200). Palladium crystallite sizes were calculated by Debye-Scherrer equation.

2.5 Electrochemical measurements

The electrochemical studies were carried out in a three-electrode cell, in all the cases, the auxiliary electrode was a platinum rod introduced into a separate porous-glass compartment. The working electrode was carbon film (nCFE), supported on glassy carbon (GC) which serves as current collector. Deposition of copper particles was carried out from an electrolytic bath; $5x10^{-2}$M $CuCl_2$, 1 M NH_4OH, 1M KCl at pH=10, in this case the Hg/HgO/1M KOH electrode was used as reference electrode. In order to evaluate the catalytic behavior, were obtained electrodes with different copper quantities (Cu/nCFE) applying a constant pulse potential of -0.772 V vs. Hg/HgO/1M KOH at 500 rpm at different time. Voltammetric measurements were conducted in 0.1 M $KHCO_3/CO_2$ at pH= 6.8, saturated with CO_2 and N_2, and the potential range applied was -1.5 to 0.1 V vs SCE, scan rate 150 mVs^{-1}.

Palladium particles were obtained from 10^{-3}M $PdCl_2$ / 1M NH_4Cl pH=0, in this case saturated calomel electrode (SCE) was used as reference. Cyclic voltammetry studies were carried out at 20 mVs^{-1} were initiated at a potential of null current ($E_{i=0}$ = 0.19V vs. SCE) in the negative direction at a potential range -0.35 to 0.65 V vs. SCE. Chronoamperometric studies were performed using potential pulses within an interval of -0.25 to 0.0 V vs. SCE. The study was always initiated applying a potential pulse in negative direction for 30 s, and later on anodic stripping voltammetry was performed at 10

mVs^{-1}, from E_{ap} toward 0.65 V in just the supporting electrolyte 1M NH_4Cl, pH=0. All solutions were prepared using analytical grade reagents and purified water from a Millipore Milli-Q system (conductivity ≤0.1 μScm^{-1}). The electrochemical measurements were performed at room temperature in AUTOLAB-PGSTAT320N with the GPES software.

3. RESULTS AND DISCUSSION

3.1 Characterization of carbon film electrodes by FTIR and SEM

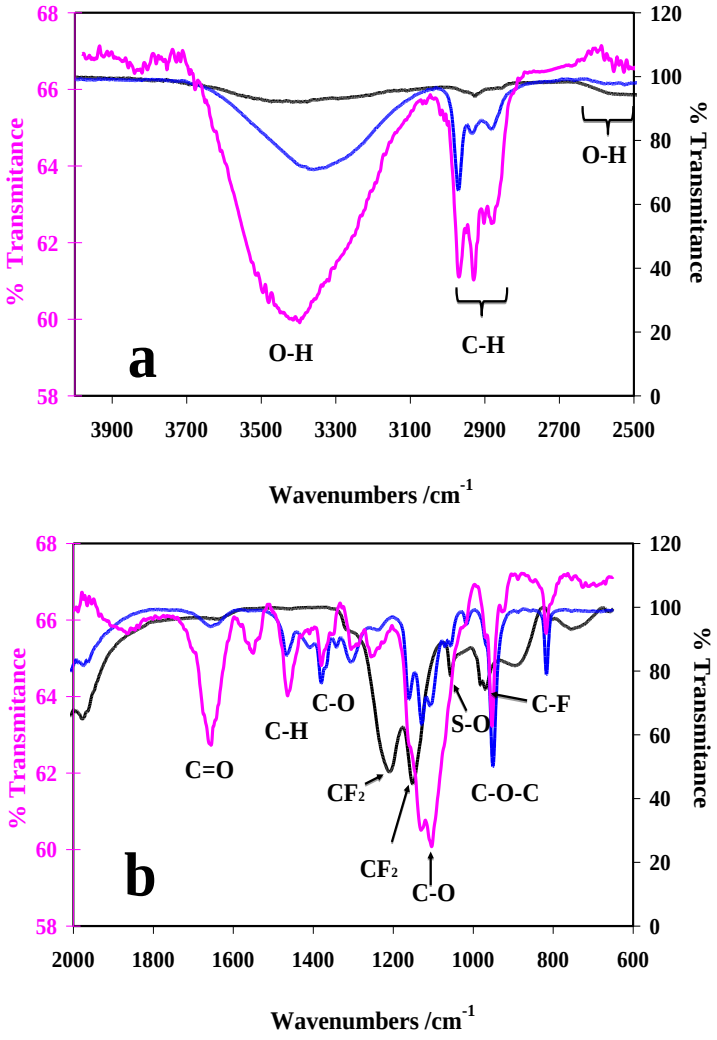

Figure 1. FTIR spectra of carbon black powder (pink line), Nafion (black line) and nCFE (blue line). The different functional groups are indicated in the figure.

The chemical surface composition of carbon film electrode, (nCFE) was evaluated from FTIR analysis. Figure 1 shows the comparison of the transmitance responses corresponding to: nanostructured carbon black in powder (pink line), Nafion, used as binder (black line) and the film

nCFE (blue line). In order to describe in more detail the functional groups present, the FTIR responses at different scales are shown (figure 1a-b). The peaks due to the vibrations and stretching of different bonds to corresponding functional groups can be observed in 3500 to 2500 cm^{-1}, and is shown in figure 1a. The figure 1b shows the vibrations and stretching bonds in the range 2000 to 600 cm^{-1} [23-25]. Taking into account the responses of Figure 1, the functional groups present in the film electrode correspond to carbon black and the Nafion. This analysis shows that the chemical composition of the film is very diverse, due to the presence of different functional groups, which give a degree of chemical reactivity.

The carbon film was supported on glassy carbon (as current collector); Figure 2 shows the images corresponding to the support material and the film. The purpose of showing the GC and the carbon film is only to compare the surfaces before and after putting the black film of carbon, the film shows spherical particles and agglomerates, which makes him look porous.

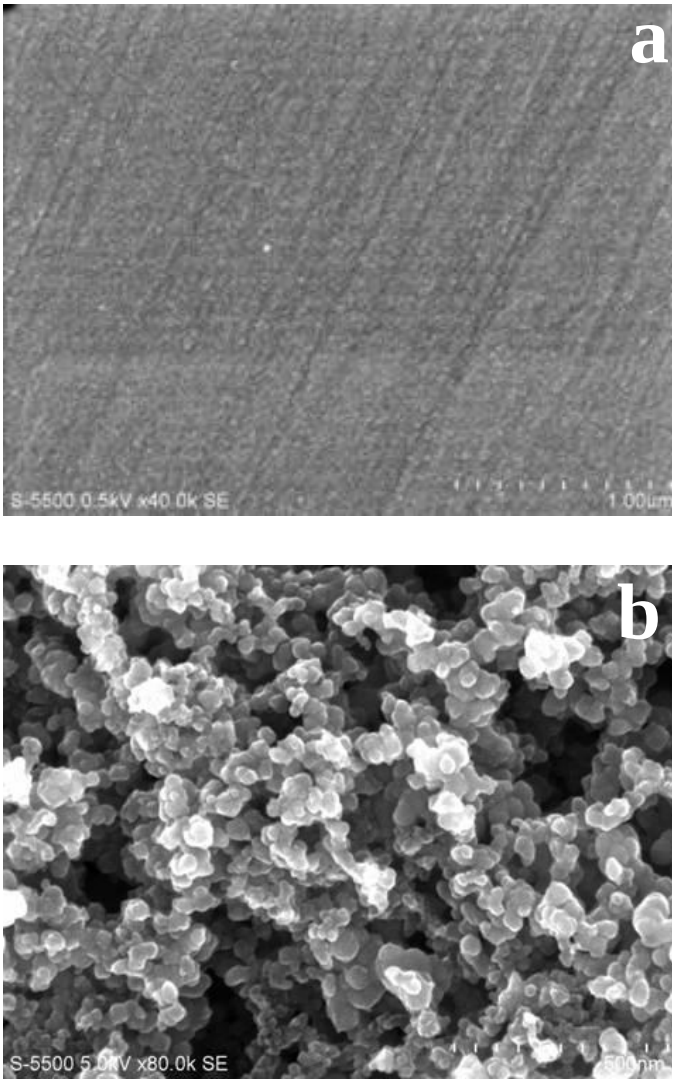

Figure 2. SEM images show the characteristic surface morphology for different carbon electrode substrates: a) glassy carbon (GC), b) carbon film electrode (nCFE).

3.2 Electrodeposits of copper on nCFE

Figure 3 shows the comparison of the cyclic voltammograms obtained on carbon film electrode (nCFE) and glassy carbon , in an electrolyte of $5x10^{-2}$ M Cu (II); 1 M NH_4OH, 1M KCl at pH=10 at 20 mVs^{-1}, in the potential range between -1.022 to 0.5 V vs. Hg/HgO/1M KOH. The sweep potential was always initiated in the negative direction from the potential of null current. In this figure showed that the reduction processes of copper are carried out in two steps: the former (Red_1) is associated to reduction of the species Cu(II) to Cu(I) and Red_2 process corresponds to the reduction Cu(I) to metallic copper, described by reactions 1 and 2 respectively and reported in [26, 27].

$$Cu(NH_3)_4^{2+} + e^- \rightleftarrows Cu(NH_3)_2^{+} + 2NH_3 \quad (1)$$

$$Cu(NH_3)_2^{+} + e^- \rightleftarrows Cu^o + 2NH_3 \quad (2)$$

When it is inversed the potential sweep direction, is defined the oxidation of the metallic copper by a wide anodic peak (Ox), this behavior it is associated to the formation of different oxides from Cu(I), as already it has been reported in [28-29]. Considering the responses of different electrodes, it is observed that the potential, for the reduction and oxidation processes depend on the nature of the substrate.

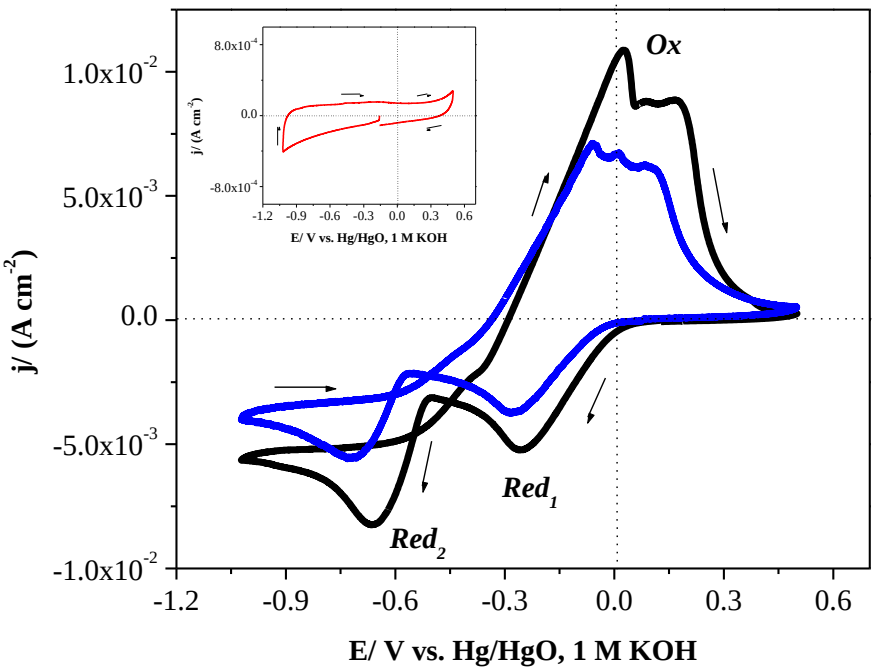

Figura 3. Comparison of the cyclic voltammetry obtained in an electrolyte of $5x10^{-2}$ M Cu (II); 1 M NH_4OH, 1M KCl at pH=10 at 20 mVs^{-1}, correspond to nCFE and glassy carbon, in the potential range between -1.022 to 0.5 V vs. Hg/HgO/1M KOH. The in-set shows the responses obtaining in support electrolyte 1M NH_4OH, 1 M KCl correspond to nCFE.

Comparing these responses with obtained in system 1M NH_4OH, 1 M KCl (supporting electrolyte) corresponding to nCFE (figure 3 the in-set) it is showed that the functional groups present in the carbon film do not interfere with the electrochemical response of processes described.

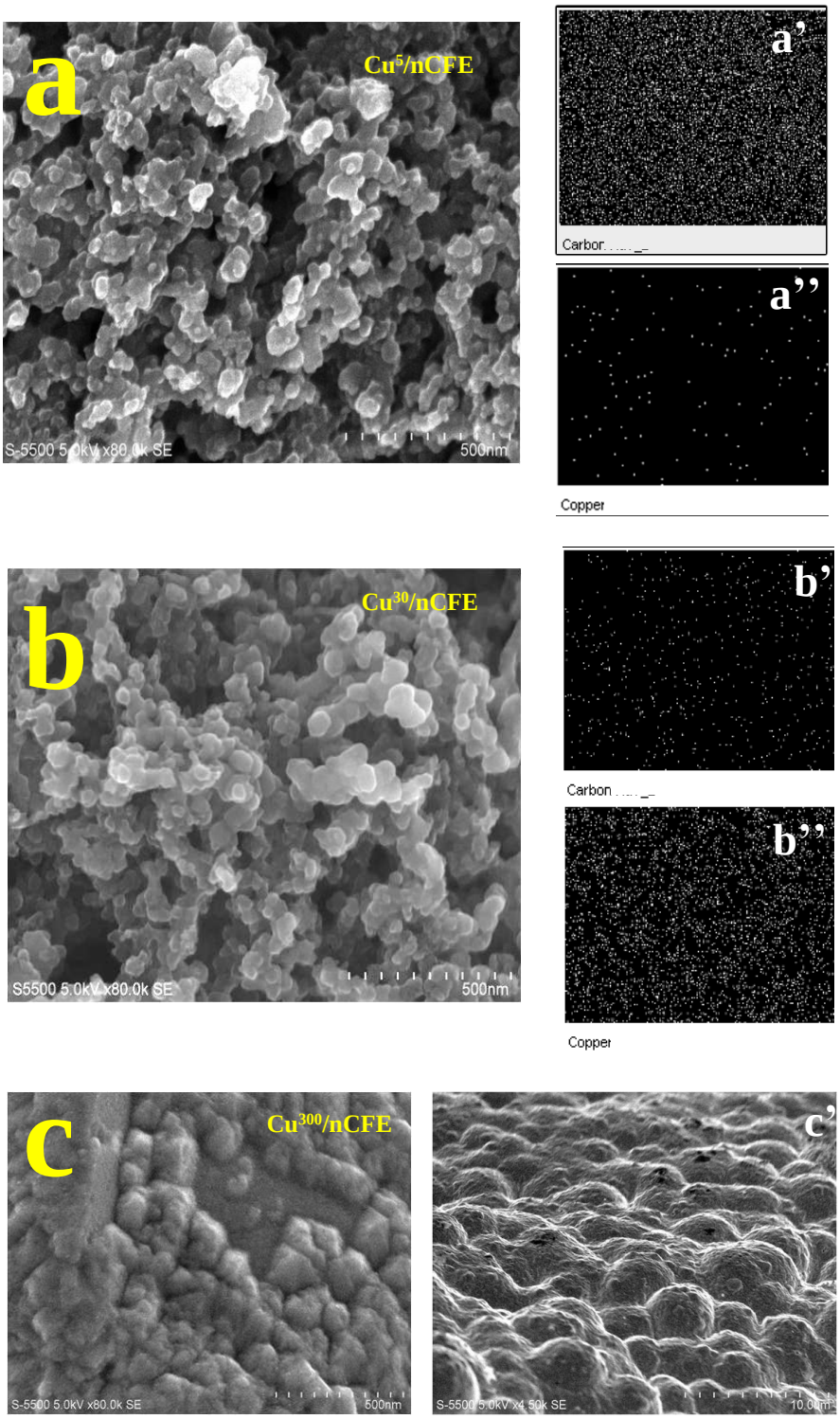

Figura 4. SEM images of the copper deposit, obtained in an electrolyte of $5x10^{-2}$ M Cu (II); 1 M NH_4OH, 1M KCl at pH=10 by applying potential pulse of -0.772 V vs. Hg/ HgO/ 1 M KOH, 500 rpm for (a-a´´) 5 s, (b-b´´) 30 s, and (c-c') 300s.

Considering the results of Figure 3 for deposit of copper on electrode nCFE we selected the potential value -0.772 V vs. Hg/HgO/1M KOH for deposit metallic copper as a function of time, in order to obtained different quantity of copper.

Figure 4a-c shows SEM images obtained at the same magnification (x80.0k) and scales (500 nm). Images in figure 4a and 4b, show spherical and agglomerate particles very similar to the image corresponding to nCFE (figure 2b), is important to note that is not evident the presence of copper. The dispersion copper on the surface of carbon electrode was analyzed by energy dispersive spectrometer (EDS) shows in figures 4a'-a''and 4b'-b'', as result of the contribution of signals characteristic X-ray of elements. These signals come from both surface and volume the analysis area. This technique confirms the dispersion copper on the surface of carbon electrode when applied pulse potential -0.772 V at short times, these particles adopt the morphology of the substrate. Metallic particles forming aggregates with uniform size on the substrate was obtained to time greater than 60 s as shown in figure 4b-c (300 s of deposit). These results allow selecting the conditions for obtained: dispersed particles, aggregates, and polycrystalline surfaces.

3.3 Cu/nCFE electrodes and their electrocatalytic behavior for electrochemical reduction of CO_2

The cyclic voltammetric was used to evaluate the catalytic behavior of the electrodes Cu/nCFE in the electrochemical reduction of CO_2. The Figure 5 shows the current-potential response correspond to electrodes with different amounts of copper. Cyclic voltammetry was performed in the potential range between -1.9 to 0.1 V vs. SCE, with a scan rate of 150 mVs^{-1} in a solution with 0.1 M $KHCO_3$, pH= 6.8 saturated with N_2 and CO_2. The responses corresponding to N_2 atmosphere, shows charge transfer processes in the limits of the potential range -1.1 to 0.1 V, this is due to oxidation and reduction of electrolytic medium (figure 5a, blue line). Electrodes with greater amount of copper, copper carbonate chemically are formed on the electrode surface [30, 31]. When it starts the potential sweep, is observe the reduction of copper carbonate in Red_1 and Red'_1 (Fig. 5b, blue line). After the direction of the potential sweep is reversed, an anodic peak (Ox) is observed, and corresponding to oxidation of the copper metal.

In CO_2 atmosphere (figure 5, red line), the response shows the reduction processes (Red_1) as discussed above, corresponding to of copper carbonate. After, a second process is described (Red_2) in -1.3 V vs SCE associated with the reduction of CO_2 [13, 32-34], this maximum increases when the amount of copper is also higher. These responses show that the copper particles supported on nCFE, have electrocatalytic ability to reduce CO_2.

On the other hand, the figure 6 shows the comparison of the responses of current-potential correspond to nCFE, Cu/nCFE, and a copper disc electrode, obtained in 0.1 M $KHCO_3$, pH = 6.8, that confirms the well catalytic behavior of the copper particles supported on nCFE; similar to described in Figure 5. Likewise, it is observed that the electrode with a higher amount of copper shows a better catalytic behavior than the copper disc electrode. This probably indicated that the adsorption of intermediate products such as CO, may interacting with the carbon support, so that the catalytic

material does not poisoning due to an important effect of the morphology (compare, in-set on figure 6 with figure 4c).

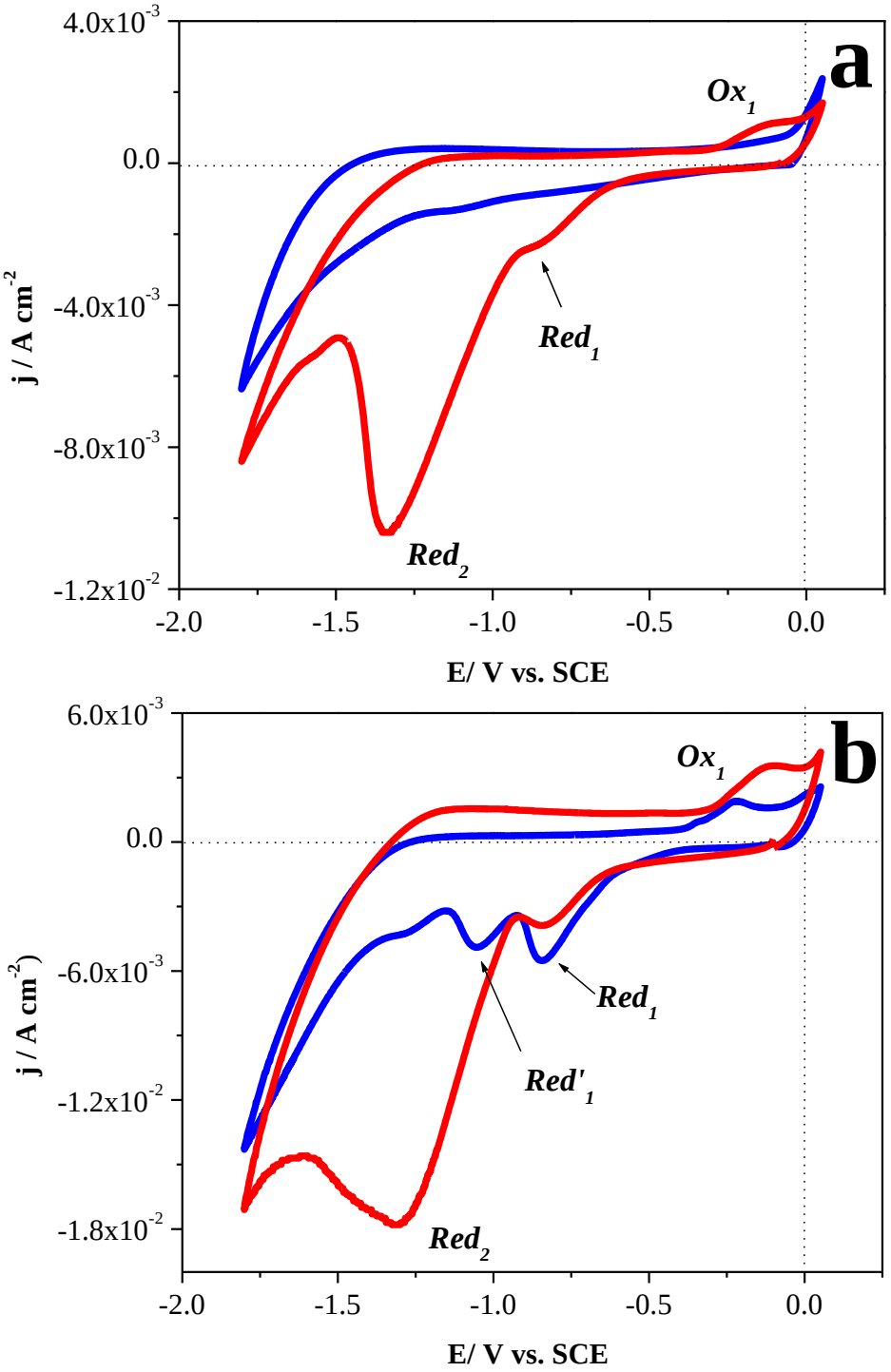

Figure 5. Comparison of voltammetric responses obtained at 150 mVs^{-1} in a solution with 0.1 M $KHCO_3$, corresponding to Cu/nCFE, to evaluated their electrocatalytic behavior. a) Cu^{60}(1.8 μg) /nCFE y b) Cu^{180}(25 μg)/ nCFE. Blue line: N_2 atmosphere, red line: CO_2 atmosphere; the copper mass was evaluated by anodic stripping voltammetry [35].

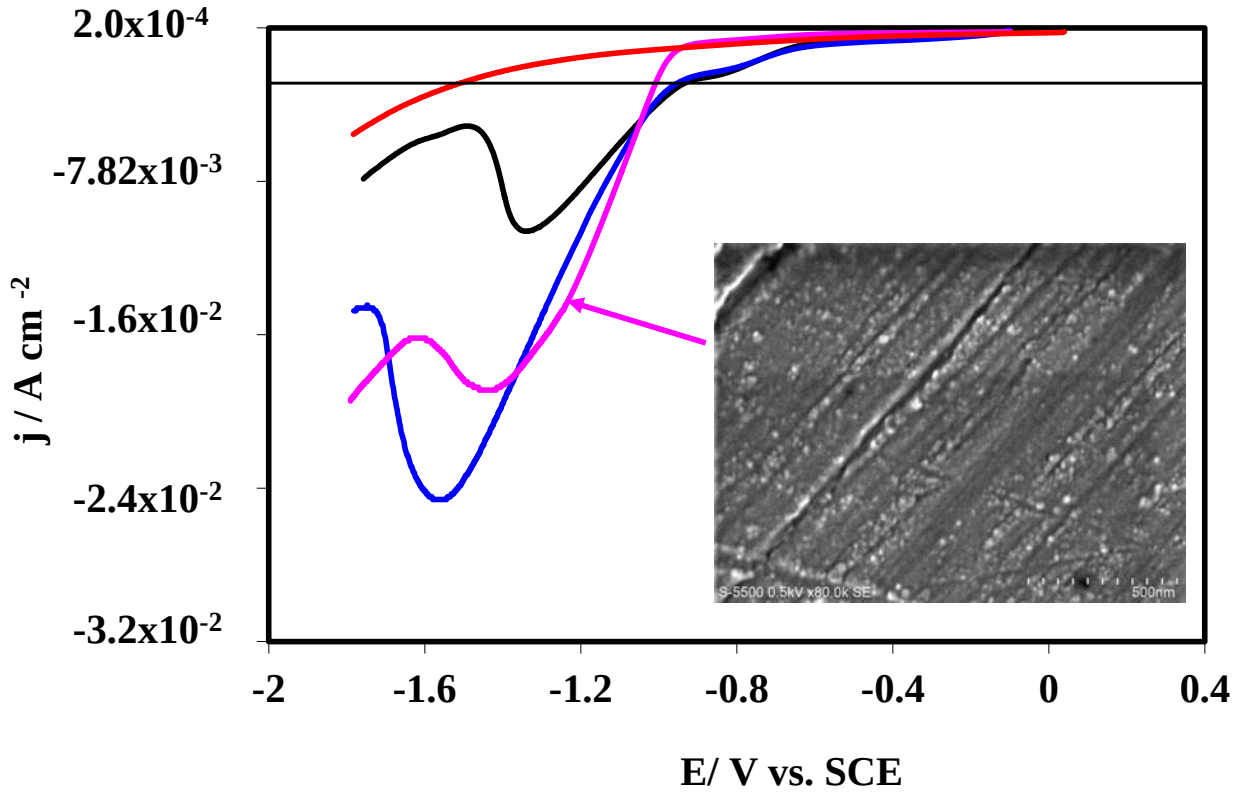

Figure 6. Comparison of voltammetric responses obtained at 150 mVs^{-1} in a solution with 0.1 M $KHCO_3$, in CO_2 atmosphere; nCFE (red line), Cu(1.8µ)/nCFE (black line), copper disc electrode (pink line), Cu(30µ)/nCFE (blue line). The copper mass was evaluated by anodic stripping voltammetry [35]. The in-set correspond to SEM image of copper disk.

3.4 Electrodeposits of palladium on nCFE

In order to characterize the electrochemical response, the figure 7 shows a comparison of the cyclic voltammograms obtained in 10^{-3}M $PdCl_2$ / 1M NH_4Cl pH=0 at 20 mVs^{-1} for nCFE and GC electrode. It is observed, that the processes of reduction and oxidation in different potential ranges; depending of substrate type. The process Red_1 corresponds to formation of metallic palladium on nCFE and GC. This process in nCFE occur at more negative potentials (-0.119 V) than in GC. Red_2 is associated to evolution of molecular hydrogen at -0.35 V for nCFE. In GC is observed the adsorption atomic hydrogen on metallic palladium (small shoulder m) in -0.23V. Oxidation processes, 1 and 2 correspond to desorption of molecular hydrogen and dissolution of metallic palladium respectively, and m' correspond to desorption of atomic hydrogen. The formation of metallic palladium has been reported in this 10^{-3}M $PdCl_2$ / 1M NH_4Cl pH=0 electrolytic system, where $PdCl_4^{2-}$ is the electroactive specie [17, 36-38] and is defined by the reaction 3:

$$PdCl_4^{2-} + 2\bar{e} \overset{\leftarrow}{\rightarrow} Pd^0 + 4Cl^- \qquad (3)$$

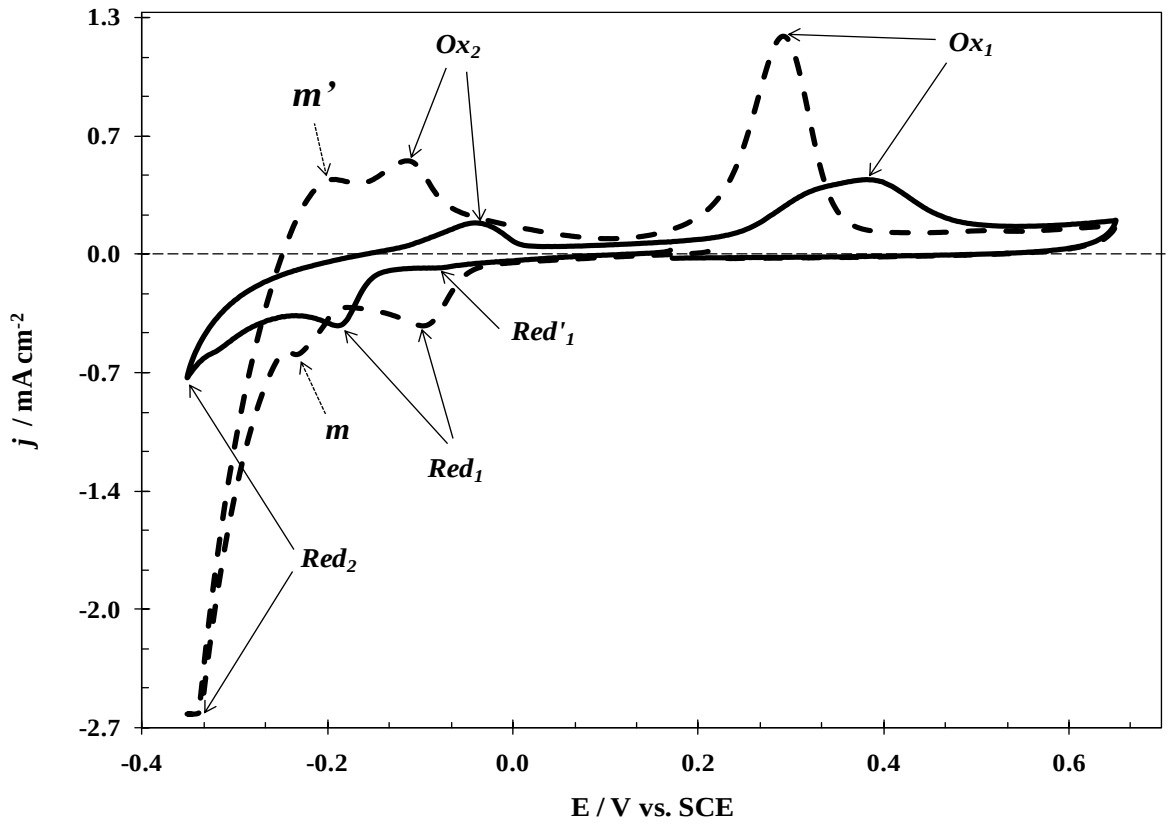

Figure 7. Comparison of the voltammograms correspond to GC (broken line) and nCFE (solid line) in the system 10^{-3}M $PdCl_2$ / 1M NH_4Cl pH=0 at 20 mVs^{-1}.

This study allows defining a range of potential for the palladium electrodeposition with and without hydrogen discharge of -0.09 V to -0.19 V and -0, 21 to -0.35 V, respectively.

A chronoamperometric study was carried out in order to confirm the range potential to obtained metallic palladium without influence of hydrogen evolution. Different potential pulses were applied, figure 8 shows (in-set) potentiostatic current transients obtained in 10^{-3}M $PdCl_2$ / 1M NH_4Cl pH=0 system with different direct potential pulses (E_{ap}) between 0.0 and -0.25 V vs. SCE during 30 s.

Later, an anodic stripping voltammetry was performed at 10 mVs^{-1}, from E_{ap} toward 0.65 V in just the supporting electrolyte 1M NH_4Cl, pH=0; the arrows in the figure indicated the sweep direction. The charge associated to palladium deposit and hydrogen adsorption was evaluated by integration of the current during the anodic potential sweep at 10 mVs^{-1}. In the responses where hydrogen adsorption occurs, the charge was evaluated in the potential range between E_{ap} to 0.19 V vs. SCE and for palladium deposit from 0.19 V to 0.65 V vs. SCE. Figure 9 shows the mass corresponding to the palladium electrodeposition and the H_2 adsorption. It is important to observe, that in all potential range applied the mass of the metallic palladium increase, this indicated that the electrodeposition of this metal continuous coupling to the hydrogen discharge. This study allows confirm a range of potential for the palladium electrodeposition with and without hydrogen discharge.

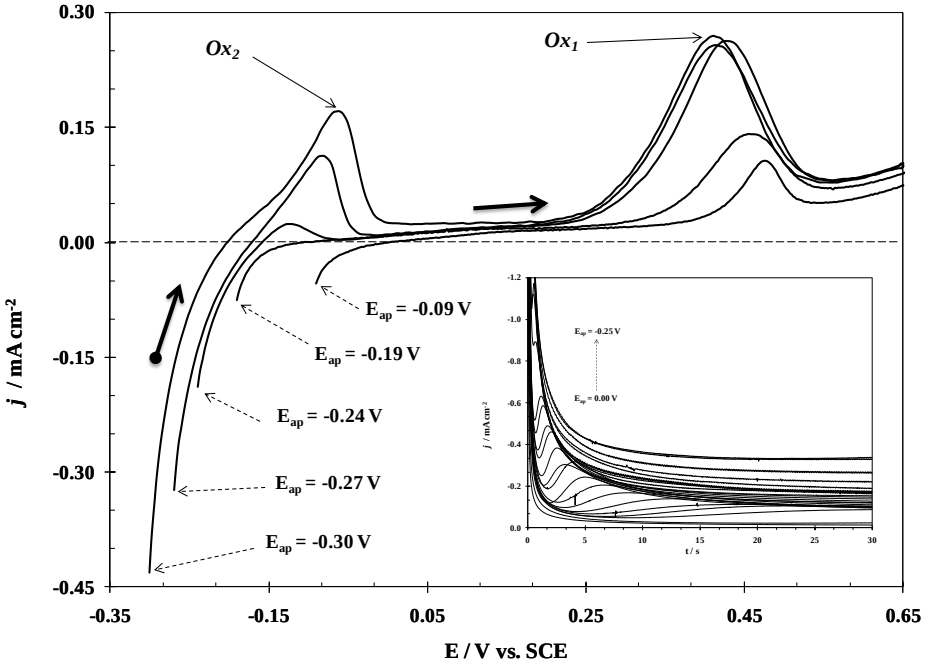

Figure 8. Potentiostatic current transients obtained in 10^{-3}M $PdCl_2$ / 1M NH_4Cl pH=0 system in different direct potential pulses (E_{ap}) between 0.00 and -0.25 V vs. SCE for 30 s for the palladium electrodeposition (in-set) and the anodic stripping voltammetry in the supporting electrolyte 1M NH_4Cl, pH=0, on the nCFE.

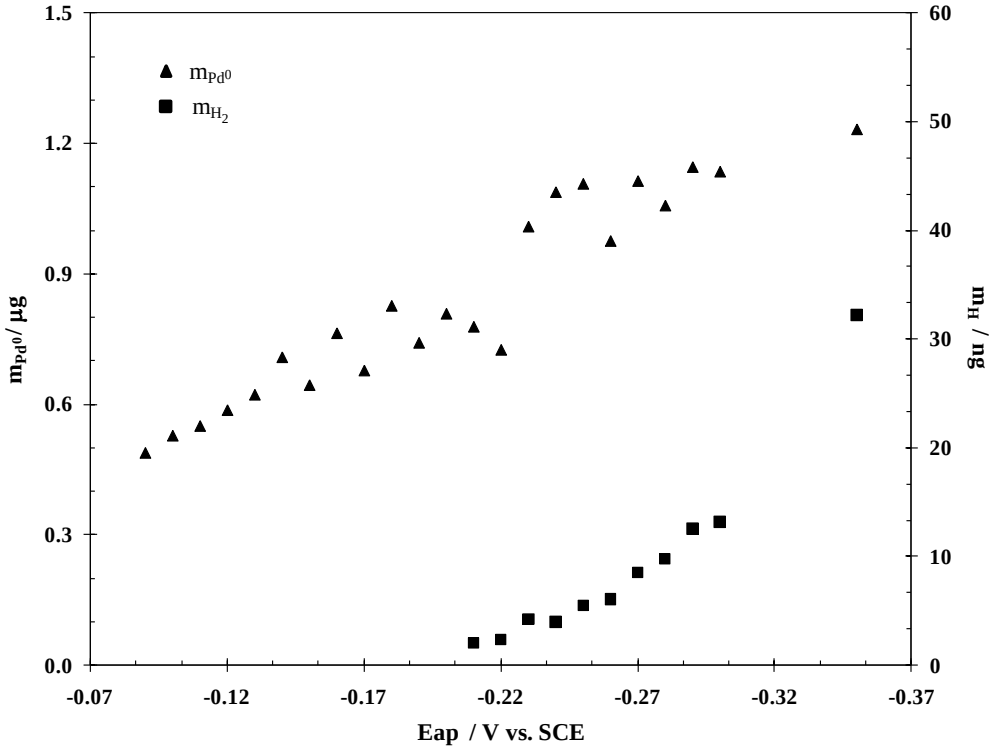

Figure 9. Mass evaluated from the responses in the figure 8, the charges were evaluated by integration of the current in anodic stripping voltammetry studies and Faraday laws for the metallic palladium and adsorbed hydrogen.

The figures 10 and 11, show of SEM images of palladium deposits obtained at -0.09 V (without hydrogen discharge) and -0.19 V (with hydrogen discharge) respectively, in the system 10^{-3}M $PdCl_2$ / 1M NH_4Cl pH=0, at different times. In general, it is observed two different morphologies; one of them is small spherical particles obtained in the potential without hydrogen discharge. In this case, the deposits were obtained in two different times and the morphology not changes; only increased the particles size. On the other hand, large crystals of palladium were observed, in hydrogen evolution potential, is clearly that the size increased of crystals is a function of deposit time. Comparing these figures is evident that the hydrogen discharge has an important influence in the morphology of palladium deposit.

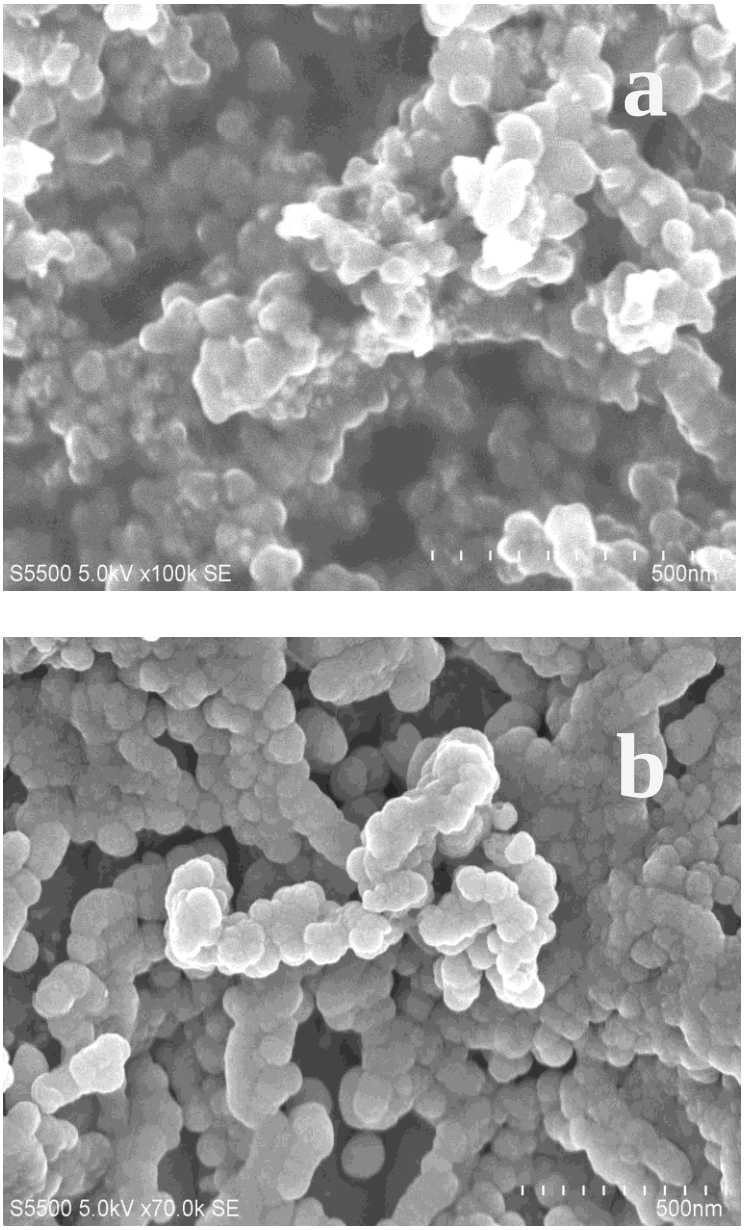

Figure 10. SEM images of palladium deposits on nCFE were obtained at -0.09 V vs. SCE in the system 10^{-3}M $PdCl_2$ / 1M NH_4Cl pH=0: a) 30 s and b) 300 s.

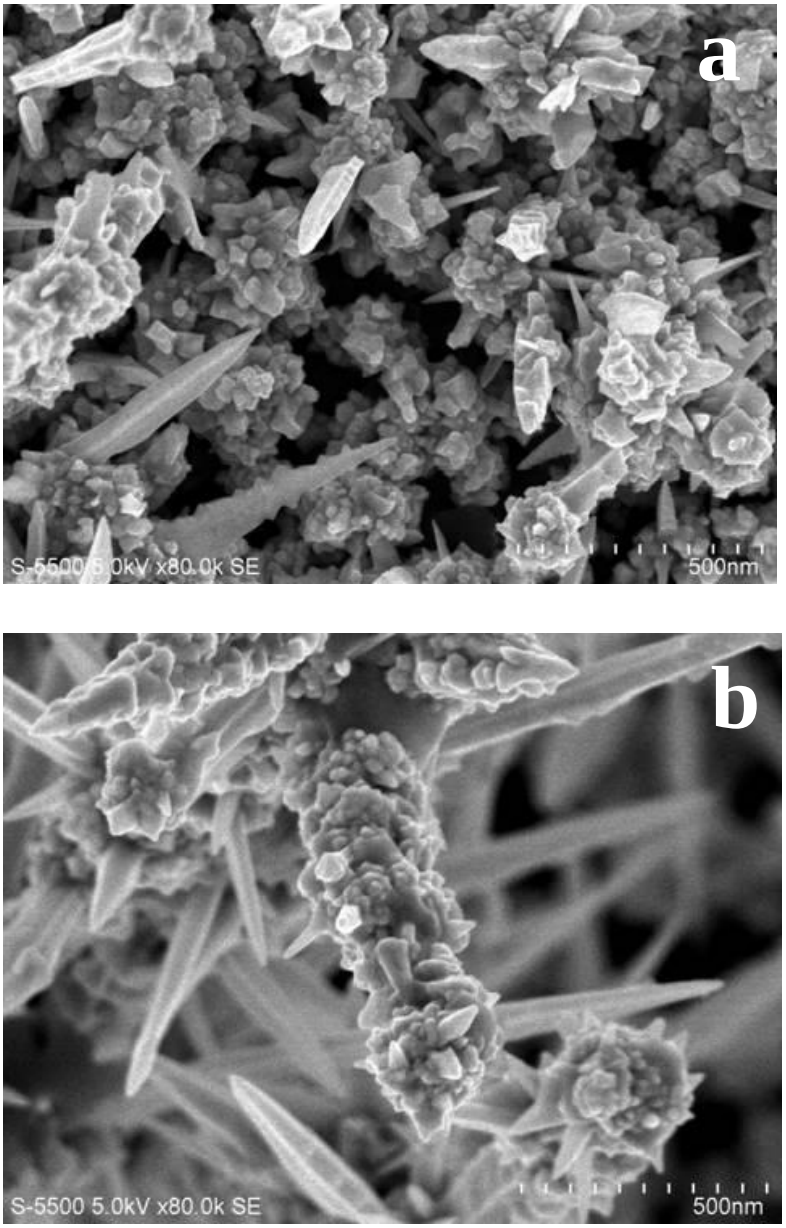

Figure 11. SEM images of palladium deposits on nCFE were obtained at -0.19 V vs. SCE in the system 10^{-3}M $PdCl_2$ / 1M NH_4Cl pH=0: a) 300 s and b) 600 s.

In order to evaluate the size of palladium particles, was carried out XRD analysis, the figure 12 shows patterns corresponding to 300 and 600 s for deposits obtained at -0.19 V vs. SCE. In this figure is showed a typical peak of amorphous carbon support in 2θ=23.27º. These electrodes exhibits diffraction lines corresponding to the (1 1 1), (2 0 0), (2 2 0) and (3 1 1) planes of a fcc (face centered cubic) palladium crystalline structure (card 46-1043). In addition, it is revealed an increasing trend in peak intensity as function of deposit time. Considering, the most intense peak (1 1 1), it was using Debye-Sherrer equation [39] and was obtained; 31 nm for deposit to 300 s and 34 nm for deposit to 600 s.

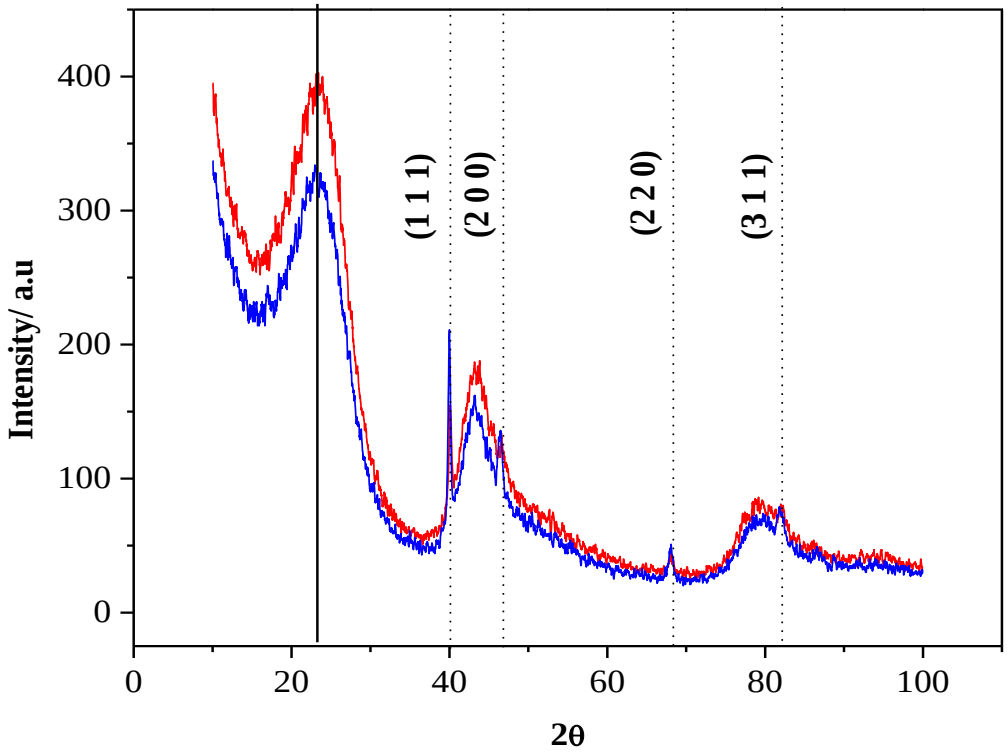

Figure 12. XRD spectrum of palladium deposits on nCFE were obtained at -0.19 V vs. SCE in the system 10^{-3}M $PdCl_2$ / 1M NH_4Cl pH=0: a) 300 s (red line), and b) 600 s (blue line).

4. CONCLUSIONS

In this study, we used commercial carbon black without prior purification, as support for catalysts. FTIR analysis shows the surface chemical composition (C-O, C=O, CF_2, CF, S-O, C-O-C), these groups provide a degree of chemical reactivity. However, they did not affect the electrochemical deposit of copper and palladium, they are not electroactive in ammonia acidic and basic systems.

By mean of cyclic voltammetry was possible to establish of the potential range of copper deposit. Such that, varying the deposit time is obtains dispersed particles, agglomerates and massive deposits, applying a constant potential. The electrodes, prepared under these conditions, were evaluated in the electrochemical reduction reaction of CO_2, and show a good behavior as catalysts, and considering the results obtained by SEM is possible to evaluate the influence of morphology in the process.

By mean of study the cyclic voltammetry and anodic stripping voltammetry were established the potential range of palladium deposit without the influence of the hydrogen evolution reaction, this is important because is possible to control the morphology of the deposit.

In summary, this paper presents an experimental methodology that we allow to establish the conditions to prepare catalyst of copper and palladium (dispersed particles, agglomerates or massive deposits) on the carbon black. The variables of potential and time, allows the control of the amount of

catalyst deposited on a low-cost commercial support, this has a significant and economic impact on the preparation of catalytic materials.

ACKNOWLEDGEMENTS
This work was financially supported by DGAPA-UNAM (IN110506-3), S.J. Figueroa Ramírez acknowledge CONACyT for scholarship. The authors thank R. Morán Elvira and René Guardian Tapia for SEM-EDS of CIICAp, María Luisa Ramon García for technical assistance in DRX analysis.

References

1. V. S. Bagotsky, *Fundamentals of Electrochemistry,* John Wiley & Sons, Inc., New Jersey and Canada (2006).
2. A. Doménech-Carbó, *Electrochemistry of Porous Materials*, CRC Press, United States of American (2009).
3. E. Furimsky, *Carbons and Carbon-Supported, Catalysts Hydroprocessing*, RSC Catalysis Series, Cambridge (2008).
4. P. Kim, Y. Kim, C. Kim, H.Kim, Y. Park, J. H. Lee, I. K.Song, J. Yi, *Catal. Lett.,* 89 (2003) 3.
5. P. Serp, J. L. Figueiredo, *Carbon Materials for catalysis, John* Wiley & Sons, Inc., New Jersey and Canada (2009).
6. A. Alouche. *Jordan Journal of Mechanical and Industrial Engineering*, 2 (2008) 111.
7. L. Lloyd, *Handbook of Industrial Catalysts. Fundamental and Applied Catalysis.* Springer, New York London (2011).
8. T. A. Ntho, *Catalytic oxidation of carbon monoxide and dimethyl ether synthesis over gold-containing catalysts,* Doctoral Thesis, University of the Witwatersrand, Johannesburg (2008).
9. J.K. Brennan, T.J. Bandosz, K.T. Thomson, K.E. Gubbins, *Colloids Surf. A.*, 187 (2001) 539.
10. V.V. Turov, V.M. Gun'ko, R. Leboda, J. Skubiszewska-Zieba, D. Palijczuk, T.J. Bandosz, Tomaszewski, S. Zietek, *J. Colloid Interface Sci*. 253 (2002) 23.
11. M.M. Dubinin, V.V. Serpinsky, *Carbon*, 19 (1981) 402.
12. Y. Hori, H. Konishi, T. Futamura, A. Murata, O. Koga, H. Sakurai and K. Oguma, *Electrochim. Acta*, 50 (2005) 5354.
13. M. Gattrell, N. Gupta, A. Co., *J. Electroanal. Chem.*, 594 (2006) 1.
14. J. Tsuji, *Palladium Reagents and Catalysts: Innovations in Organic Synthesis*, John Wiley & Sons, Ltd, Chichester, UK, (1996).
15. R. S. Jayashree, J.S. Spendelow, J. Yeom, C. Rastogi, M.A. Shannon, P.J.A. Kenis, *Electrochim. Acta*, 50 (2005) 4674.
16. P. Bruzzoni, R.M. Carranza, J.R. Lacoste, *Jornadas SAM-CONAMET-AAS*, (2001) 1149.
17. D.N. Escobar-Muñoz, A.K. Cuentas-Gallegos, M. Miranda-Hernández, *Theoretical and Experimental Advances in Electrodeposition*, Research Signpost, India (2008).
18. V.C. Diculescu, A.M. Chiorcea, *J. Solid State Electrochem.*, 11 (2007) 887.
19. M.H. Martin, A. Lasia, *Electrochim. Acta*, 53 (2008) 6317.
20. V.C. Diculesco, A.M. Chiorcea-Paquim, O. Corduneanu, *J. Solid State Electrochem.*, 11 (2007) 887.
21. W. L. Lewis, *Platinum Metals*, 26 (1967) 20.
22. J. Kleperis, G. Wójcik and A. Czerwinski, *J. Solid State Electrochem.*, 5 (2001) 229.
23. K. Kinoshita, *Carbon. Electrochemical and Physicochemical Properties*, John Wiley & Sons Inc., New York (1988).
24. R. T. Conley. *Espectroscopia Infrarroja*, Alhambra, Madrid, España (1979).

25. M. S. Shafeeyan, W. M. A. W. Daud, A. Houshmand, A. Shamiri, *J. Anal. Appl. Pyrolysis,* 89 (2010) 143.
26. S. J. Figueroa Ramírez, M. Miranda Hernández, *ECS Transactions-23rd Meeting of The Mexican Electrochemical Society*, 15 (2008) 181.
27. A. Ramos, M. Miranda-Hernandez, I. Gonzalez, *J. Electrochem. Soc.*, 148 4 (2001) C315.
28. C.Nila, I. González, *J. Electronal.Chem*., 401 (1996) 171.
29. C.Nila, I. González, *Hydrometallurgy*, 47 (1996) 63.
30. L.M. Gassa, A.M. Castro Luna, R.M. Torres Sánchez, J.O. Zerbino., *Portugaliae Electrochimica Acta,* 22 (2004) 81.
31. M. Pérez Sánchez, M. Barrera, S. González, R.M. Souto., *Electrochemica Acta,* 35 9 (1990) 1337.
32. C.G. Vayenas, Modern Aspect of Electrochemistry No.42, Springer, New York (2008).
33. Y. Hori, A. Murata, R. Takahashi, *J. Chem. Soc., Faraday Trans.*, 1 85 8 (1989) 2309.
34. H. Cardona, C. Moral, C.R. Cabrera, *J. Electroanal. Chem*., 513 (2001) 45.
35. S. J. Figueroa Ramírez, M. Miranda Hernández, A study Voltammetric of deposition and anodic stripping of copper on nanostructured carbon in ammonia bath (in preparation).
36. C.D. Tait, D.R. Janecky, P.S.Z. Rogers, *Geochim. Cosmochim. AC.*, 55 (1991) 1253.
37. J.J. Cruywagen, R.J. Kriek, *J. Coord. Chem.*, 60, (2007) 439.
38. A.H. Sanchez Peña, M. Miranda Hernández, *ECS Transactions-24th Meeting of The Mexican Electrochemical Society*, 20 1 (2009) 365.
39. C. Hammond, *The Basics of Crystallography and Diffraction*, International Union of Crystallography, New York (2009).